Modeling of Semibatch Styrene Suspension Polymerization Processes

Marcelo Kaminski Lenzi,[1,2] Michael F. Cunningham,[2] Enrique Luis Lima,[1] José Carlos Pinto[1]

[1]*Universidade Federal do Rio de Janeiro, Programa de Engenharia Química/COPPE, Cidade Universitária, Rio de Janeiro 21945-970, RJ, Brasil*
[2]*Queen's University, Department of Chemical Engineering, 19 Division Street, K7L 3N6 Kingston, Ontario, Canada*

Received 19 May 2004; accepted 17 November 2004
DOI 10.1002/app.21652
Published online in Wiley InterScience (www.interscience.wiley.com).

ABSTRACT: We developed a mathematical model to describe the behavior of semibatch styrene suspension polymerization processes, where the constituents of a typical emulsion polymerization process are added into the reaction vessel during the course of a typical suspension reaction. This technique was recently described for the production of core–shell polymer particles. The model assumes that the nucleated emulsion particles can agglomerate with the sticky and much bigger suspension particles and that the agglomeration rate constant is a function of the internal states of the suspended droplets. The proposed model presented good agreement with experimental conversion, average molecular weight, and molecular weight distribution data. © 2005 Wiley Periodicals, Inc. J Appl Polym Sci 96: 1950–1967, 2005

Key words: emulsion polymerization; modeling; molecular weight distribution/molar mass distribution

INTRODUCTION

A large number of experimental techniques have been used successfully for the production of polymer resins with broad/bimodal molecular weight distributions (MWDs). This goal may be achieved by the sudden modification of the concentrations of chain-transfer agents,[1,2] the modification of reactor operation conditions,[3] or polymerization with mixtures of different catalysts.[4] Broad MWDs can also be produced through the blending of different polymer resins during the final processing stage. However, in this case, the final performance of the polymer material may be affected by the much less efficient mixing of the polymer chains. Therefore, there are incentives to produce polymer materials with broad MWDs at the reaction stage.

In the first article of this series, an alternative technique was developed for the production of broad/bimodal MWD polymer resins.[5] The developed technique consists of a semibatch suspension polymerization process where the components of a conventional emulsion polymerization recipe are fed into the reaction vessel during the course of a typical suspension polymerization process. The reported experimental data show that by the variation of the moment when the emulsion process charge is added into the reactor, both the MWD and the particle morphology can be changed, allowing for the formation of core–shell polymer structures and bimodal MWDs.

Extensive modeling studies have been carried out for polymerization processes.[6] An ideal model for a polymerization process should be able to predict the end-use properties of the polymer resin as a function of the operation conditions.[7] However, for most polymerization processes, this type of model is not available yet. The large majority of modeling and control studies have been devoted to the prediction of the molecular properties of the final polymer resin. Mathematical models that are able to predict the particle size distribution,[8] MWD,[9] and copolymer composition[10] of polymer materials have been successfully reported. As these models can be used for both the design of polymer materials and the control of the final polymer characteristics, there are huge incentives for the development of accurate mathematical models for polymerization processes.

Suspension polymerization processes are characterized by the use of monomers that are insoluble in a continuous phase, generally water, and by the fact that monomer droplets are dispersed in the continuous phase through a combination of strong agitation and the use of suspending agents.[11] Polymerization starts when an oil-soluble initiator is added to the system. Polymerization reactions occur inside the stabilized monomer droplets, which can be considered microre-

Correspondence to: J. C. Pinto (pinto@peq.coppe.ufrj.br).
Contract grant sponsor: Coordenação de Aperfeiçoamento de Pessoal de Nível Superior.
Contract grant sponsor: Conselho Nacional de Desenvolvimento Científico e Tecnológico.
Contract grant sponsor: Fundação Carlos Chagas Filho de Amparo à Pesquisa do Estado do Rio de Janeiro.
Contract grant sponsor: Queen's University.

actors. For this reason, the polymerization kinetics are similar to the kinetics of the bulk polymerization system.[6] Polymerizations usually follow a free-radical mechanism, and the average particle size of the final polymer particle lies within the interval of 10 μm to 5 mm. As the polymer particles contain a very large number of radicals, the average molecular weights of the final product are normally much lower than the average molecular weights of resins prepared in emulsion.[12] Further details regarding the modeling of suspension polymerization processes can be found elsewhere.[13–15]

Emulsion polymerization processes are also characterized by the use of a continuous phase, generally water. However, contrary to suspension polymerization systems, emulsifiers simultaneously stabilize the monomer droplets and form micelles, which nucleate the polymer particles, the main loci of the polymerization. Besides, the initiator is normally soluble in the aqueous phase, so that complex mass-transfer steps may take place during the reaction course.[16] According to the classical mechanism,[17] polymer particle nucleation occurs in the first stage of the polymerization, when radicals formed in the aqueous phase either enter a monomer swollen micelle (micellar nucleation) or precipitate after reaching a critical size (homogeneous nucleation).[18] As the size of the monomer droplets is much larger (1–100 μm) than the size of the micelles (1–10 nm) and the final polymer particles (ca. 100 nm), radicals generated in the aqueous phase are captured mostly by the micelles and the polymer particles, the main loci of the polymerization, whereas monomer droplets act as raw material reservoirs. The second stage begins when the particle nucleation is finished. At this stage, the concentration of monomer inside polymer particles is kept essentially constant. When the monomer droplets disappear, the third stage begins, and the polymerization continues until the complete depletion of the monomer. The final product of the polymerization is a latex with particle size typically ranging from 100 to 1000 nm.[18] Because of its compartmentalized character, emulsion polymerization processes can simultaneously present high reaction rates and products with high average molecular weights. Also, the final product can eventually be used in the latex form, with no need for an additional separation stage.[19] The classical work of Smith and Ewart,[20] dealing with the 0–1 kinetics, was the first attempt to model the emulsion polymerization process. Min and Ray[21] presented a very detailed mathematical model for emulsion reactions, considering complex kinetic phenomena such as homogeneous nucleation, particle breakage, and particle coalescence. Recently, Saldivar et al.[22] and Gao and Penlidis[16] presented detailed mathematical models for emulsion copolymerization processes.

Our main objective in this article is to present a mathematical model for styrene semibatch suspension processes, when the constituents of a typical emulsion recipe are fed into the reaction vessel during the course of a typical suspension polymerization reaction. The mathematical model was validated with experimental data reported by Lenzi et al.[23] The modeling approach is based on models reported previously for suspension and emulsion processes. The main feature of these semibatch suspension processes is the formation of a core–shell structure, which is taken into account by the assumption that part of the emulsified polymer material is captured by the suspended polymer particles, in accordance with a first-order rate of agglomeration. The captured polymer material forms the particle shell, whereas the original suspended droplets form the particle core. We show that the mathematical model is able to describe the evolution of the experimental monomer conversion and molecular weight averages very successfully. Also, the mathematical model is also able to predict the evolution of the full MWD of the polymer resin very accurately.

MATHEMATICAL MODELING

The semibatch suspension polymerization process presents features of typical emulsion and suspension polymerizations. For instance, during the first moments of a semibatch reaction, the polymerization follows a typical suspension polymerization scheme. After the initiation of the monomer feeding, polymerization reactions occur simultaneously inside the suspended and the emulsified polymer particles. For this reason, it is convenient to present and validate the modeling approaches used to describe the emulsion and suspension polymerizations before the presentation of the detailed mathematical model used to describe the semibatch polymerization process.

Modeling of the conventional emulsion polymerization process

The mathematical model developed to describe the emulsion polymerization process comprises a set of differential–algebraic equations. Model equations were derived by assuming that

1. The reactor is perfectly mixed.
2. Reactions occur under isothermal conditions.
3. Particle coalescence and particle breakage do not occur in the polymer particle level.
4. Initiator decomposition occurs in the aqueous phase, and polymerization reactions occur inside the polymer particles.

TABLE I
Mechanisms for the Emulsion Polymerization Reaction

Initiator decomposition	$I \xrightarrow{k_d^{emu}} 2R^{\bullet}$
Particle nucleation	$R^{\bullet} + \text{mic} \rightarrow P_1$
Radical entry in a particle with no growing radical	$R^{\bullet} + \text{Part} \rightarrow P_1$
Radical entry in a particle containing a growing radical	$R^{\bullet} + P_n \rightarrow \Theta_n$
Propagation	$P_n + M \xrightarrow{k_p} P_{n+1}$
Chain transfer to monomer	$M + P_m \xrightarrow{k_{tf\_mon}} \Theta_m + P_1$

I = initiator; $R^{\bullet}$ = radical formed by initiator decomposition; mic = micelle; Part = polymer particle of the emulsion process containing no growing polymer chains; P_n = growing polymer radical with a chain size equal to n; Θ_n = polymer chain with a chain size equal to n; M = monomer.

5. The compartmentalization of growing radicals can be described by the classical 0–1 polymerization kinetics.[20]
6. Radical desorption from polymer particles does not occur.
7. Particle nucleation occurs through micellar nucleation.
8. Kinetic parameters do not depend on the chain size.
9. Monomer concentrations inside the monomer droplets and polymer particles are in equilibrium. (However, to allow for more efficient implementation of the numerical code, mass balance equations were derived with nonequilibrium conditions.)
10. Radicals originated by initiator decomposition and chain transfer to monomer have similar reactivity.

The reaction mechanism used to describe the polymerization kinetics is presented in Table I. Chain-transfer reactions to monomer were considered to be the unique type of chain-transfer reactions to occur.

The initiator decomposition is considered to be a first-order rate process and can be described by eq. (1). As mentioned before, micellar nucleation is responsible for the formation of new polymer particles. Therefore, the number of particles is given by eq. (2), which assumes that the probability of an existing radical to enter a micelle is proportional to the relative micellar interfacial area of the overall population of micelles and polymer particles:

$$\frac{dI}{dt} = -k_d^{\text{emu}} I \tag{1}$$

$$\frac{dN_P}{dt} = (2f_{\text{emu}} k_d^{\text{emu}} I)\left(\frac{N_{\text{mic}} a_{\text{mic}}}{N_{\text{mic}} a_{\text{mic}} + N_P a_P}\right) \tag{2}$$

where I is the number of moles of initiator, t is the time (s), k_d^{emu} is the water-soluble initiator decomposition rate constant (1/s), f_{emu} is the water-soluble initiator efficiency, N_{mic} is the number of micelles, a_{mic} is the surface area of the micelle, N_P is the number of polymer particles formed in the emulsion polymerization process, and a_P is the surface area of a polymer particle of the emulsion polymerization process (cm^2).

We also assumed that the partitioning of emulsifier among the many phases that constitute the reaction medium follows a priority order. The surfactant first covers the polymer particles; the remaining emulsifier molecules saturate the aqueous phase; and finally, the remaining amount of emulsifier forms the micelles. The amount of surfactant needed to cover the monomer droplets is considerably smaller than the amount needed to cover the polymer particles. This is mainly due to the low interfacial area of the monomer droplets. Further details can be found elsewhere.[24]

Monomer can be found in three phases of the reaction medium: the aqueous phase, the polymer particles, and the monomer droplets. Equations (3)–(5) present the monomer mass balances for each of these phases. The equilibrium concentrations were calculated with monomer partition coefficients, as reported in the literature.[25] For simulation purposes, mass-transfer coefficients were assumed to be very large so that monomer concentrations were at equilibrium:

$$\frac{dM_{\text{Part}}}{dt} = -r_P^{\text{emu}} + km_{\text{Part-AQ}} a_{\text{Part-AQ}}([M_{\text{Part}}] - [M_{\text{Part}}^{\text{EQ}}]) \tag{3}$$

$$\frac{dM_{\text{AQ}}}{dt} = -km_{\text{Part-AQ}} a_{\text{Part-AQ}}([M_{\text{AQ}}] - [M_{\text{AQ}}^{\text{EQ}}]) - km_{\text{mon-AQ}} a_{\text{mon-AQ}}([M_{\text{AQ}}] - [M_{\text{AQ}}^{\text{EQ}}]) \tag{4}$$

$$\frac{dM_{\text{mon}}}{dt} = M_{\text{FEED}} + km_{\text{mon-AQ}} a_{\text{mon-AQ}}([M_{\text{mon}}] - [M_{\text{mon}}^{\text{EQ}}]) \tag{5}$$

where M_ϕ is the number of moles of monomer in the phase ϕ, where ϕ is the monomer, polymer particles, or aqueous phase; r_P^{emu} is the propagation rate of the emulsion polymerization process (mol $cm^{-3} \cdot s^{-1}$); $km_{\text{Part-AQ}}$ is the monomer mass-transfer coefficient between the polymer particles and aqueous phase in the emulsion polymerization process (cm/s); $[M_\phi]$ is the monomer concentration in the phase ϕ, where ϕ is the monomer, polymer particles, or aqueous phase (if the superscript EQ is present, this indicates the equilib-

rium monomer concentration in the phase indicated by the mass-transfer coefficient; mol/cm^3); $a_{\text{Part–AQ}}$ is the interfacial area between the polymer particle and the aqueous phase and monomer droplets in the emulsion polymerization process (cm^2); $km_{\text{mon–AQ}}$ is the monomer mass-transfer coefficient between the monomer droplets and aqueous phase in the emulsion polymerization process (cm/s); $a_{\text{mon–AQ}}$ is the interfacial area between the aqueous phase and the monomer droplets in the emulsion polymerization process (cm^2); and M_{FEED} is the monomer feed flow rate.

The polymerization rate is given by eq. (6). We derived eq. (6) by considering that the emulsion polymerization kinetics follows the classical 0–1 system. Therefore, the average number of growing radicals per polymer particle is equal to 0.5:

$$r_P^{\text{emu}} = k_P[M_{\text{Part}}]\left(\frac{\bar{n}N_P}{N_A}\right) = k_P[M_{\text{Part}}]\left(\frac{0.5N_P}{N_A}\right) \qquad (6)$$

where k_P is the propagation rate constant (cm^3 mol^{-1} s^{-1}), n is the average number of growing radicals per particle of the emulsion polymerization process, and N_A is Avogadro's number.

The model equations used to describe the molecular weight averages were derived with the classical moments technique.[26] Pseudosteady state was assumed for growing radicals. Equations (7) and (8) present the kth-order moments for growing radicals and dead polymer chains, respectively, based on the kinetic mechanism presented in Table I.

$$\begin{aligned}\frac{d\mu_k}{dt} = &-(k_P/V_{\text{Pol}})M_{\text{Part}}\mu_k + (k_P/V_{\text{Pol}})M_{\text{Part}}\sum_{i=1}^{\infty}(i+1)^k P_i \\ &- (k_{\text{tf\_mon}}/V_{\text{Pol}})M_{\text{Part}}\mu_k + (k_{\text{tf\_mon}}/V_{\text{Pol}})M_{\text{Part}}\mu_0 \\ &- 2f_{\text{emu}}k_d^{\text{emu}}I\left[\frac{\bar{n}a_PN_P}{a_{\text{mic}}N_{\text{mic}} + a_PN_P}\right]\left[\frac{\mu_k}{\bar{n}N_P}\right] \\ &+ 2f_{\text{emu}}k_d^{\text{emu}}I\left[\frac{a_{\text{mic}}N_{\text{mic}} + \bar{n}a_PN_P}{a_{\text{mic}}N_{\text{mic}} + a_PN_P}\right] \qquad (7)\end{aligned}$$

$$\begin{aligned}\frac{d\lambda_k}{dt} = &(k_{\text{tf\_mon}}/V_{\text{Pol}})M_{\text{Part}}\mu_k + 2f_{\text{emu}}k_d^{\text{emu}}I\left[\frac{\bar{n}a_PN_P}{a_{\text{mic}}N_{\text{mic}} + a_PN_P}\right] \\ &\times\left[\frac{\mu_k}{\bar{n}N_P}\right] \qquad (8)\end{aligned}$$

where μ_k is the kth-order moment of the growing polymer chain distribution, V_{Pol} is the volume of the polymer phase of the emulsion polymerization process (cm^3), P_i is the number of moles of growing polymer radicals with a chain size equal to i, $k_{\text{tf\_mon}}$ is the chain transfer to monomer rate constant (cm^3 mol^{-1} · s^{-1}), and λ_k is the kth-order moment of the dead polymer chain distribution.

One should observe that μ_0 and λ_0 describe the overall molar concentrations of live and dead polymer chains, respectively, whereas μ_1 and λ_1 describe the overall molar concentrations of mers in live and dead polymer chains, respectively. The higher order moments do not have physical meaning but can be used for the computation of the main statistical properties of the MWDs of the live and dead polymer chains.[26]

The shape of the MWD cannot be recovered just through computation of the molecular weight averages.[26] It is also well known that the shape of the MWD significantly influences the end-use properties of the polymer resin; therefore, the mathematical model becomes a more efficient and reliable tool if it can predict the full MWD. The approach used here for MWD calculation is similar to the one reported by Kiparissides et al.[27] based on the computation of the mass balances of each individual dead polymer chain. However, to improve the efficiency of the numerical scheme, the population of growing polymer chains was assumed to follow the Flory distribution.[28] Therefore

$$\begin{aligned}\frac{d\Theta_n}{dt} = &(k_{\text{tf\_mon}}/V_{\text{Pol}})M_{\text{Part}}\mu_0(1-q)q^{n-1} \\ &+ 2f_{\text{emu}}k_d^{\text{emu}}I\left[\frac{\bar{n}a_PN_P}{a_{\text{mic}}N_{\text{mic}} + a_PN_P}\right]\left[\frac{\mu_0(1-q)q^{n-1}}{\bar{n}N_P}\right] \qquad (9)\end{aligned}$$

where Θ is the number of moles of polymer, n is the chain length, and q is Flory's probability of propagation and is equal to $q = \bar{\imath}-1/\bar{\imath}$, $\bar{\imath}=\mu_1/\mu_0$. q is the propagation probability and i is the number-average chain size of the MWD of live polymer chains, calculated in terms of the leading statistical moments, and is equal to μ_1/μ_0.

Modeling of the conventional suspension polymerization process

Because of the larger size, polymer particles formed in the suspension process may contain a large number of growing radicals;[13] consequently, the compartmentalized character of the polymer particles is lost, and each monomer droplet can be regarded as a microreactor. For this reason, the kinetic behavior of the suspension process is similar to the kinetic behavior of a bulk polymerization process.[6] The following assumptions were also made for model derivation:

1. The reactor is perfectly mixed.
2. Reactions are performed under isothermal conditions.
3. Reactions do not occur in the aqueous phase.

TABLE II
Mechanism for the Suspension Polymerization Reaction

Initiator decomposition	$I \xrightarrow{k_d^{susp}} 2R^{\bullet}$
	$R^{\bullet} + M \rightarrow P_1$
Propagation	$P_n + M \xrightarrow{k_P} P_{n+1}$
Chain transfer to monomer	$M + P_m \xrightarrow{k_{tf\_mon}} \Theta_m + P_1$
Termination by combination	$P_n + P_m \xrightarrow{k_{t\_comb}} \Theta_{n+m}$

I = initiator; $R^{\bullet}$ = radical formed by initiator decomposition; M = monomer; P_n = growing polymer radical with a chain size equal to n; Θ_n = polymer chain with a chain size equal to n.

4. The initiator is present only in the organic phase.
5. Radical desorption from polymer particles does not occur.
6. Kinetic parameters do not depend on the chain size.
7. Radicals originated by initiator decomposition and chain transfer to monomer have similar reactivity.

The reaction mechanism used for the derivation of the mathematical model is presented in Table II. Again, chain-transfer reactions to monomer were considered to be the unique type of chain-transfer reactions to occur.

As a droplet-by-droplet modeling approach is not necessary, the mathematical model of the suspension polymerization process is simpler than the model of the emulsion polymerization process. The rate of initiator decomposition can be considered as a first-order rate process described by eq. (10). The monomer balance is given by eq. (11). The propagation rate was derived by consideration of the long-chain hypothesis and is given by eq. (12):

$$\frac{dI}{dt} = -k_d^{\text{susp}} I \tag{10}$$

$$\frac{dM}{dt} = -r_P^{\text{susp}} V_{\text{org}} \tag{11}$$

$$r_P^{\text{susp}} = k_P[M]\sqrt{\frac{2f_{\text{susp}}k_d^{\text{susp}}[I]}{k_{\text{t\_comb}}}} \tag{12}$$

where k_d^{susp} is the oil-soluble initiator decomposition rate constant (1/s), M is the number of moles of monomer, r_P^{susp} is the propagation rate of the bulk/suspension polymerization process (mol cm^{-3} · s^{-1}), V_{org} is the volume of the organic phase of the suspension/bulk polymerization process (cm^3), [M] is the monomer concentration, f_{susp} is the oil-soluble initiator efficiency, [I] is the initiator concentration, and $k_{\text{t\_comb}}$ is the termination by combination rate constant (cm^3 mol^{-1} · s^{-1}).

The moments technique is also used here to calculate the molecular weight averages. The leading moments of the growing polymer chains distribution can be obtained by eq. (13), whereas eq. (14) can be used to derive the leading moments of the dead polymer chain distribution. The pseudo-steady-state hypothesis can be used for deriving the moment equations for the growing polymer chains:

$$\frac{d\mu_k}{dt} = 2f_{\text{susp}}k_d^{\text{susp}}I - (k_P/V_{\text{org}})M\mu_k + (k_P/V_{\text{org}})M\sum_{i=1}^{\infty}(i+1)^k P_i - (k_{\text{tf\_mon}}/V_{\text{org}})M\mu_k - (k_{\text{t\_comb}}/V_{\text{org}})\mu_k\mu_0 + (k_{\text{tf\_mon}}/V_{\text{org}})M\mu_0 \tag{13}$$

$$\frac{d\lambda_k}{dt} = (k_{\text{tf\_mon}}/V_{\text{org}})M\mu_k + [k_{\text{t\_comb}}/(2V_{\text{org}})]\sum_{n=1}^{\infty}P_n\sum_{i=1}^{\infty}(n+i)^k P_i \tag{14}$$

The full MWD of the polymer produced by the suspension process can be calculated as in the emulsion polymerization process. The assumptions previously used are also considered valid for the suspension process. Equation (15) presents the mass balance for dead polymer chains of size n:

$$\frac{d\Theta_n}{dt} = (k_{\text{tf\_mon}}/V_{\text{org}})M\mu_0(1-q)q^{n-1} + [k_{\text{t\_comb}}/(2V_{\text{org}})]\mu_0\mu_0(1-q)^2(n-1)q^{n-2} \tag{15}$$

Modeling of the semibatch suspension polymerization process

The semibatch suspension polymerization process studied here is not conventional because the constituents of a typical emulsion polymerization process are charged into the reaction vessel during the course of a previously started suspension polymerization. So, it is worth dividing the model into two parts. The first part comprises only the suspension polymerization process and can be described by eqs. (10)–(15). The second part of the model

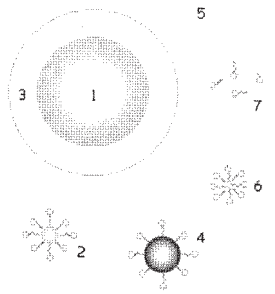

Figure 1 Components of the reaction medium in the second part of the semibatch polymerization process

requires that both the suspension and emulsion polymerization processes be taken into account as they are performed simultaneously inside the same reaction vessel. The experimental results obtained by Lenzi et al.[23] clearly show that the two processes are not independent and interact with each other. This conclusion is based on the formation of the core–shell structure and on changes of the molecular weight averages during the course of the polymerization.

Figure 1 illustrates the distinct phases of the reaction medium during the second part of the semibatch suspension polymerization process, when feeding of the emulsion components is started. The presence of (1) polymer beads produced in the first reaction step, (2) polymer particles formed by the emulsion polymerization process, (4) monomer droplets, (5) water, (6) micelles, and (7) free surfactant is shown. A third polymeric phase (3) is formed through agglomeration of the emulsified polymer particles over the previously formed polymer beads originated by the suspension polymerization process. It must be emphasized that this agglomeration process originates the core–shell morphology of the final product.

All of the assumptions used previously to describe the conventional emulsion and suspension polymerization processes are assumed to remain valid. However, some additional hypotheses need to be considered because of the interaction between both of the polymerization processes:

1. The compartmentalization character of the polymer particles formed by the emulsion polymerization process is lost when these particles are captured by the polymer beads formed by the suspension polymerization process.
2. Mass transfer is allowed between the core (1) and the shell (3) of the polymer beads.
3. The agglomeration phenomena can be described as a first-order rate process. The parameter of the emulsion polymer particle agglomeration process [k_{NP} (1/s)] was used to describe this first-order rate equation. Therefore, the higher the value of k_{NP} is, the higher the rate of agglomeration among suspended and emulsified polymer particles will be.

It is important to emphasize that agglomeration is assumed to occur among emulsified polymer particles over the polymer particles previously formed by the suspension process, as observed experimentally. The agglomeration rates are expected to depend on the overall interfacial surface formed between the suspended polymer beads and the continuous aqueous phase, on the characteristics of the interface (interfacial tension, viscosity, etc.), and on the mixing conditions (agitation speed, shear rates, vessel geometry, etc.). As a first attempt to describe the agglomeration phenomena, these details are completely neglected, and k_{NP} is assumed to be constant throughout the batch (although k_{NP} is allowed to vary from batch to batch). This is in accordance with the assumptions that the overall interfacial surface, surface characteristics, and mixing conditions do not change significantly after the startup of the emulsion feeding. As shown in the next paragraphs, these assumptions, although very simple, allow for proper interpretation of available experimental data.

The reaction mechanism used for derivation of the mathematical model of the second reaction step is presented in Table III. The mechanism considers that the polymerization reactions occur in three distinct polymer phases: the polymer beads formed by the suspension process (phase I), the polymer particles formed by the emulsion polymerization process (phase II) and the shell formed by the agglomeration process (phase III). The other phases present in the reactor are the raw monomer droplets (phase IV) and the water (phase V).

The initiator and monomer mass balances in each of the phases present in the reactor are given by eqs. (16)–(18) and (19)–(23), respectively. Attention must be paid to the following points:

1. The initiator used for the emulsion process cannot initiate polymer chains in the suspended particles.
2. Equilibrium concentrations are obtained with the aid of partition coefficients.
3. The agglomeration process is represented in eqs. (20) and (21) by the rate terms, which are multiplied by k_{NP}.

$$\frac{dI^{I}}{dt} = -k_d^{susp} I^{I} - ki_{I-III} a_{I-III}([I^{I}] - [I^{I-EQ}]) \qquad (16)$$

$$\frac{dI^{III}}{dt} = -k_d^{susp} I^{III} + ki_{I-III} a_{I-III}([I^{III}] - [I^{III-EQ}]) \qquad (17)$$

TABLE III
Mechanism for the Semibatch Suspension Polymerization Reaction

Initiator decomposition	$I^{\mathrm{I,III}} \xrightarrow{k_d^{\mathrm{susp}}} 2R^{\bullet\mathrm{I,III}}$
	$R^{\bullet\mathrm{I,III}} + M^{\mathrm{I,III}} \rightarrow P_1^{\mathrm{I,III}}$
Propagation	$P_n^{\mathrm{I,III}} + M^{\mathrm{I,III}} \xrightarrow{k_P} P_{n+1}^{\mathrm{I,III}}$
Chain transfer to monomer	$M^{\mathrm{I,III}} + P_m^{\mathrm{I,III}} \xrightarrow{k_{\mathrm{tf\_mon}}} \Theta_m^{\mathrm{I,III}} + P_1^{\mathrm{I,III}}$
Termination by combination	$P_n^{\mathrm{I,III}} + P_m^{\mathrm{I,III}} \xrightarrow{k_{\mathrm{t\_comb}}} \Theta_{n+m}^{\mathrm{I,III}}$
Initiator decomposition	$I^{\mathrm{V}} \xrightarrow{k_d^{\mathrm{emu}}} 2R^{\bullet\mathrm{V}}$
Particle nucleation	$R^{\bullet\mathrm{V}} + \mathrm{mic} \rightarrow P_1^{\mathrm{II}}$
Radical entry in a particle with no growing radical	$R^{\bullet\mathrm{V}} + \mathrm{Part} \rightarrow P_1^{\mathrm{II}}$
Radical entry in a particle containing a growing radical	$R^{\bullet\mathrm{V}} + P_n^{\mathrm{II}} \rightarrow \Theta_n$
Propagation	$P_n^{\mathrm{II}} + M^{\mathrm{II}} \xrightarrow{k_P} P_{n+1}^{\mathrm{II}}$
Chain transfer to monomer	$M^{\mathrm{II}} + P_m^{\mathrm{II}} \xrightarrow{k_{\mathrm{tf\_mon}}} \Theta_m^{\mathrm{II}} + P_1^{\mathrm{II}}$

The superscripts I–V refer to the distinct polymer phases described in the text. I = initiator; $R^{\bullet}$ = radical formed by initiator decomposition; M = monomer; P_n = growing polymer radical with a chain size equal to n; Θ_n = polymer chain with a chain size equal to n; mic = micelle; Part = polymer particle of the emulsion process containing no growing polymer chains.

$$\frac{dI^{\mathrm{V}}}{dt} = -k_d^{\mathrm{emu}} I^{\mathrm{V}} \tag{18}$$

$$\frac{dM^{\mathrm{I}}}{dt} = -r_P^{\mathrm{susp}} V^{\mathrm{I}} - km_{\mathrm{I-III}} a_{\mathrm{I-III}} ([M^{\mathrm{I}}] - [M^{\mathrm{I-EQ}}]) \tag{19}$$

$$\frac{dM^{\mathrm{II}}}{dt} = -r_P^{\mathrm{emu}} + km_{\mathrm{II-V}} a_{\mathrm{II-V}} ([M^{\mathrm{II}}] - [M^{\mathrm{V-EQ}}]) - k_{\mathrm{NP}} M^{\mathrm{II}} \tag{20}$$

$$\frac{dM^{\mathrm{III}}}{dt} = -r_P^{\mathrm{susp}} V^{\mathrm{III}} + km_{\mathrm{I-III}} a_{\mathrm{I-III}} ([M^{\mathrm{III}}] - [M^{\mathrm{III-EQ}}]) + k_{\mathrm{NP}} M^{\mathrm{II}} + km_{\mathrm{III-V}} a_{\mathrm{III-V}} ([M^{\mathrm{III}}] - [M^{\mathrm{III-EQ}}]) \tag{21}$$

$$\frac{dM^{\mathrm{IV}}}{dt} = \mathrm{FEED} + km_{\mathrm{IV-V}} a_{\mathrm{IV-V}} ([M^{\mathrm{IV}}] - [M^{\mathrm{IV-EQ}}]) \tag{22}$$

$$\frac{dM^{\mathrm{V}}}{dt} = -km_{\mathrm{IV-V}} a_{\mathrm{IV-V}} ([M^{\mathrm{V}}] - [M^{\mathrm{V-EQ}}]) - km_{\mathrm{II-V}} a_{\mathrm{II-V}} ([M^{\mathrm{V}}] - [M^{\mathrm{V-EQ}}]) - km_{\mathrm{III-V}} a_{\mathrm{III-V}} ([M^{\mathrm{V}}] - [M^{\mathrm{V-EQ}}]) \tag{23}$$

where I^{ϕ} is the number of moles of initiator in the phase ϕ, where ϕ is I, III, or V; $ki_{\mathrm{I-III}}$ is the oil-soluble initiator mass-transfer coefficient between phases I and III; $a_{\mathrm{I-III}}$ is the interfacial area between phases I and III; $[\mathrm{I}^{\phi}]$ is the initiator concentration in the phase ϕ, where ϕ is I or III (if the superscript EQ is present, this indicates the equilibrium monomer concentration in the phase indicated by the mass-transfer coefficient; mol/L); M^{ϕ} is the number of moles of monomer in the phase ϕ, where ϕ is I, II, III, IV, or V; V^{ϕ} is the volume of the phase ϕ, where ϕ is I, II, III, IV, or V (cm^3); $km_{\mathrm{I-III}}$ is the monomer mass-transfer coefficient between phases I and III (cm/s); $[\mathrm{M}^{\phi}]$ is the monomer concentration in the phase ϕ, where ϕ is I, II, III, IV, or V (if the superscript EQ is present, this indicates the equilibrium monomer concentration in the phase indicated by the mass-transfer coefficient; $\mathrm{mol/cm}^3$); $km_{\mathrm{II-V}}$ is the monomer mass-transfer coefficient between phases II and V (cm/s); $a_{\mathrm{II-V}}$ is the interfacial area between phases II and V (cm^2); $km_{\mathrm{III-V}}$ is the monomer mass-transfer coefficient between phases III and V (cm/s); $a_{\mathrm{III-V}}$ is the interfacial area between phases III and V (cm^2); $km_{\mathrm{IV-V}}$ is the monomer mass-transfer coefficient between phases IV and V (cm/s); and $a_{\mathrm{IV-V}}$ is the interfacial area between phases IV and V (cm^2).

The number of polymer particles formed by the emulsion process is given by eq. (24). The main difference from eq. (2) is the presence of the term that accounts for the loss of particles due to agglomeration, leading to the formation of the particle shell. For modeling purposes, the partition of the emulsifier among the existing phases is assumed to occur as previously described for the conventional emulsion polymerization process:

$$\frac{dN_P}{dt} = (2f_{\mathrm{emu}} k_d^{\mathrm{emu}} I^{\mathrm{V}}) \left(\frac{N_{\mathrm{mic}} a_{\mathrm{mic}}}{N_{\mathrm{mic}} a_{\mathrm{mic}} + N_P a_P} \right) - k_{\mathrm{NP}} N_P \tag{24}$$

The polymerization rates are given by eqs. (25) and (26). The kinetic behavior inside the suspension beads and the polymer shell is similar to the kinetic behavior of bulk polymerization processes. However, as concentrations in the core and in the shell are not the same, the reaction rates in both phases may be very different. On the other hand, the emulsion polymerization process follows the classical 0–1 system, with compartmentalization of the growing polymer chains:

$$r_P^{\mathrm{susp-I}} = k_P [M^{\mathrm{I}}] \sqrt{\frac{2f_{\mathrm{susp}} k_d^{\mathrm{susp}} [I^{\mathrm{I}}]}{k_{\mathrm{t\_comb}}}} \tag{25}$$

$$r_P^{\mathrm{susp-III}} = k_P [M^{\mathrm{III}}] \sqrt{\frac{2f_{\mathrm{susp}} k_d^{\mathrm{susp}} [I^{\mathrm{III}}]}{k_{\mathrm{t\_comb}}}} \tag{26}$$

$$r_P^{\mathrm{emu}} = k_P [M^{\mathrm{II}}] \left(\frac{\bar{n} N_P}{N_A} \right) = k_P [M^{\mathrm{II}}] \left(\frac{0.5 N_P}{N_A} \right) \tag{27}$$

where $r_P^{susp-\phi}$ is the propagation rate of the bulk/suspension polymerization process in the phase ϕ, where ϕ is I or III (mol cm^{-3} · s^{-1}).

The molecular weight averages were also obtained through the leading moments of the MWD of the polymer chains of phases I (polymer chains formed by the suspension polymerization process), II (polymer chains formed by the emulsion polymerization process) and III (polymer chains of the polymeric shell), as shown in eqs. (28)=(30) for growing polymer chains and eqs. (31)=(33) for dead polymer chains. Equations (29) and (30) for growing radicals and eqs. (32) and (33) are coupled because of the core–shell structure:

$$\frac{d\mu_k^{\mathrm{I}}}{dt} = 2f_{\mathrm{susp}}k_d^{\mathrm{susp}}I^{\mathrm{I}} - (k_P/V^{\mathrm{I}})M^{\mathrm{I}}\mu_k^{\mathrm{I}} + (k_P/V^{\mathrm{I}})M^{\mathrm{I}}\sum_{i=1}^{\infty}(i+1)^kP_i^{\mathrm{I}} - (k_{\mathrm{tf\_mon}}/V^{\mathrm{I}})M^{\mathrm{I}}\mu_k^{\mathrm{I}} - (k_{\mathrm{t\_comb}}/V^{\mathrm{I}})\mu_k^{\mathrm{I}}\mu_0^{\mathrm{I}} + (k_{\mathrm{tf\_mon}}/V^{\mathrm{I}})M^{\mathrm{I}}\mu_0^{\mathrm{I}} \quad (28)$$

$$\frac{d\mu_k^{\mathrm{II}}}{dt} = -(k_P/V^{\mathrm{II}})M^{\mathrm{II}}\mu_k^{\mathrm{II}} + (k_P/V^{\mathrm{II}})M^{\mathrm{II}}\sum_{i=1}^{\infty}(i+1)^kP_i^{\mathrm{II}} - (k_{\mathrm{tf\_mon}}/V^{\mathrm{II}})M^{\mathrm{II}}\mu_k^{\mathrm{II}} + (k_{\mathrm{tf\_mon}}/V^{\mathrm{II}})M^{\mathrm{II}}\mu_0^{\mathrm{II}} - 2f_{\mathrm{emu}}k_d^{\mathrm{emu}}I^{\mathrm{V}}\left[\frac{\bar{n}a_PN_P}{a_{\mathrm{mic}}N_{\mathrm{mic}}+a_PN_P}\right]\left[\frac{\mu_k^{\mathrm{II}}}{\bar{n}N_P}\right] + 2f_{\mathrm{emu}}k_d^{\mathrm{emu}}I^{\mathrm{V}}\left[\frac{a_{\mathrm{mic}}N_{\mathrm{mic}}+\bar{n}a_PN_P}{a_{\mathrm{mic}}N_{\mathrm{mic}}+a_PN_P}\right] - k_{\mathrm{NP}}\mu_k^{\mathrm{II}} \quad (29)$$

$$\frac{d\mu_k^{\mathrm{III}}}{dt} = 2f_{\mathrm{susp}}k_d^{\mathrm{susp}}I^{\mathrm{III}} - (k_P/V^{\mathrm{III}})M^{\mathrm{III}}\mu_k^{\mathrm{III}} + (k_P/V^{\mathrm{III}})M^{\mathrm{III}}\sum_{i=1}^{\infty}(i+1)^kP_i^{\mathrm{III}} - (k_{\mathrm{tf\_mon}}/V^{\mathrm{III}})M^{\mathrm{III}}\mu_k^{\mathrm{III}} - (k_{\mathrm{t\_comb}}/V^{\mathrm{III}})\mu_k^{\mathrm{III}}\mu_0^{\mathrm{III}} + (k_{\mathrm{tf\_mon}}/V^{\mathrm{III}})M^{\mathrm{III}}\mu_0^{\mathrm{III}} + k_{\mathrm{NP}}\mu_k^{\mathrm{II}} \quad (30)$$

$$\frac{d\lambda_k^{\mathrm{I}}}{dt} = (k_{\mathrm{tf\_mon}}/V^{\mathrm{I}})M^{\mathrm{I}}\mu_k^{\mathrm{I}} + [k_{\mathrm{t\_comb}}/(2V^{\mathrm{I}})]\sum_{n=1}^{\infty}P_n^{\mathrm{I}}\sum_{i=1}^{\infty}(n+i)^kP_i^{\mathrm{I}} \quad (31)$$

$$\frac{d\lambda_k^{\mathrm{II}}}{dt} = (k_{\mathrm{tf\_mon}}/V^{\mathrm{II}})M^{\mathrm{II}}\mu_k^{\mathrm{II}} + 2f_{\mathrm{emu}}k_d^{\mathrm{emu}}I^{\mathrm{V}}\left[\frac{\bar{n}a_PN_P}{a_{\mathrm{mic}}N_{\mathrm{mic}}+a_PN_P}\right]\times\left[\frac{\mu_k^{\mathrm{II}}}{\bar{n}N_P}\right] - k_{\mathrm{NP}}\lambda_K^{\mathrm{II}} \quad (32)$$

$$\frac{d\lambda_k^{\mathrm{III}}}{dt} = (k_{\mathrm{tf\_mon}}/V^{\mathrm{III}})M^{\mathrm{III}}\mu_k^{\mathrm{III}} + [k_{\mathrm{t\_comb}}/(2V^{\mathrm{III}})]\sum_{n=1}^{\infty}P_n^{\mathrm{III}}\sum_{i=1}^{\infty}(n+i)^kP_i^{\mathrm{III}} + k_{\mathrm{NP}}\lambda_n^{\mathrm{II}} \quad (33)$$

where μ_k^{ϕ} is the kth-order moment of the growing polymer chain distribution in the phase ϕ, where ϕ is I, II, or III; P_i^{ϕ} is the number of moles of growing polymer radicals with a chain size equal to i in the phase ϕ, where ϕ is I, II, or III; and λ_k^{ϕ} is the kth-order moment of the dead polymer chain distribution in the phase ϕ, where ϕ is I, II, or III.

The weight-average molecular weight (M_w; g/mol) and the number-average molecular weight (M_n; g/mol) of the final polymer resin are given by eqs. (34) and (35), respectively:

$$M_w = \frac{\lambda_2^{\mathrm{III}}+\lambda_2^{\mathrm{II}}+\lambda_2^{\mathrm{I}}}{\lambda_1^{\mathrm{III}}+\lambda_1^{\mathrm{II}}+\lambda_1^{\mathrm{I}}}PM_{\mathrm{mon}} \quad (34)$$

$$M_n = \frac{\lambda_1^{\mathrm{III}}+\lambda_1^{\mathrm{II}}+\lambda_1^{\mathrm{I}}}{\lambda_0^{\mathrm{III}}+\lambda_0^{\mathrm{II}}+\lambda_0^{\mathrm{I}}}PM_{\mathrm{mon}} \quad (35)$$

where PM_{mon} is the monomer molecular weight (g/mol).

The mathematical model is also capable of calculating the MWD of the final polymer resin. The approach used is similar to the one previously described for conventional emulsion and suspension polymerization processes. Therefore, we developed population balances for the growing and dead polymer chains of the three polymer phases by considering the agglomeration process, which is responsible for the coupling of the mass balances of phases II and III. The balance equations for phases I, II, and III are given by eqs. (36)=(38), respectively:

$$\frac{d\Theta_n^{\mathrm{I}}}{dt} = (k_{\mathrm{tf\_mon}}/V^{\mathrm{I}})M^{\mathrm{I}}\mu_0^{\mathrm{I}}(1-q^{\mathrm{I}})(q^{\mathrm{I}})^{n-1} + [k_{\mathrm{t\_comb}}/(2V^{\mathrm{I}})]\mu_0^{\mathrm{I}}\mu_0^{\mathrm{I}}(1-q^{\mathrm{I}})^2(n-1)(q^{\mathrm{I}})^{n-2} \quad (36)$$

$$\frac{d\Theta_n^{\mathrm{II}}}{dt} = (k_{\mathrm{tf\_mon}}/V^{\mathrm{II}})M^{\mathrm{II}}\mu_0^{\mathrm{II}}(1-q^{\mathrm{II}})(q^{\mathrm{II}})^{n-1} - k_{\mathrm{NP}}\Theta_n^{\mathrm{II}} + 2f_{\mathrm{emu}}k_d^{\mathrm{emu}}I^{\mathrm{II}}\left[\frac{\bar{n}a_PN_P}{a_{\mathrm{mic}}N_{\mathrm{mic}}+a_PN_P}\right]\left[\frac{\mu_0^{\mathrm{II}}(1-q^{\mathrm{II}})(q^{\mathrm{II}})^{n-1}}{\bar{n}N_P}\right] \quad (37)$$

$$\frac{d\Theta_n^{\mathrm{III}}}{dt} = (k_{\mathrm{tf\_mon}}/V^{\mathrm{III}})M^{\mathrm{III}}\mu_0^{\mathrm{III}}(1-q^{\mathrm{III}})(q^{\mathrm{III}})^{n-1} + [k_{\mathrm{t\_comb}}/(2V^{\mathrm{III}})]\mu_0^{\mathrm{III}}\mu_0^{\mathrm{III}}(1-q^{\mathrm{III}})^2(n-1)(q^{\mathrm{III}})^{n-2} + k_{\mathrm{NP}}\Theta_n^{\mathrm{II}} \quad (38)$$

TABLE IV
Kinetic Parameters

Parameter	Value	Reference
	9.0×10^{-6}	30
f_{susp}	0.6	Adjusted for this work
f_{emu}	0.6	25
k_d^{susp}	$1.7 \times 10^{14} \times e^{[-(30{,}000.0/1.987T)]}$	12
k_d^{emu}	2.0×10^{-5}	25
k_P	$1.09 \times 10^{10} \times e^{[-(7050.0/1.987T)]}$	12
k_{tf_mon}	$2.37 \times 10^{7} \times e^{[-(7816.0/1.987T)]}$	12
k_{t_comb}	$1.70 \times 10^{12} \times e^{[-(2268.0/1.987T)]}$	12

CMC = critical micelle concentration.

where Θ_n^{ϕ} is the number of moles of polymer chains with chain length n in the phase ϕ, where ϕ is I, II, or III, and where $q^{\phi} = (i^{-\phi} - 1)/i^{-\phi}$ and $i^{-\phi} = \mu_1^{\phi}/\mu_0^{\phi}$ for when the phase ϕ is I, II, or III.

The MWD of the final product is given as the sum of the polymer contents of each phase, as given in eq. (39):

$$\Theta_n^{final}(t) = \Theta_n^{III}(t) + \Theta_n^{II}(t) + \Theta_n^{I}(t) \quad (39)$$

where Θ_i^{final} is the number of moles of polymer chains with chain length i in the final product of the semibatch suspension process.

Model parameters

The developed mathematical model comprises a set of differential–algebraic equations. Model integration was performed numerically with the DASSL package.[29] The mass-transfer coefficients were set to arbitrarily high values to allow for equilibrium conditions to develop. Table IV presents the values and expressions for the kinetic parameters. The remaining parameters required for simulation of the emulsion polymerization process can be obtained in Gilbert.[25]

For proper description of the suspension polymerization process, the termination reaction constant was corrected to take the gel effect into account. An empirical equation was used to describe the gel effect, as presented in eq. (40). Model parameters were determined with the experimental conversion data of Lenzi et al.,[23] obtained for conventional styrene suspension polymerizations:

$$g = e^{[-0.1\chi - 1.2\chi^2]} \quad (40)$$

where g is the ratio between the termination rate constant at actual reaction conditions and the termination rate constant at zero monomer conversion at the same reaction temperature and χ is the monomer conversion.

Finally, k_{NP} controls the agglomeration process. A careful analysis of the experimental data presented by Lenzi et al.[23] leads to the following key conclusions about this parameter:

1. k_{NP} depends on the size of the polymer particles formed by the suspension polymerization process. The bigger the suspended particles are, the

TABLE V
Polymerization Recipes

Constituent (g)	Polymerization recipe			
	REAC01	REAC05	REAC06	REAC07
Styrene	Charged: 30.0 Pumped: 40.0	Charged (S): 100.0 Charged (E): 30.0 Pumped (E): 45.0	Charged (S): 100.0 Charged (E): 30.0 Pumped (E): 57.0	Charged (S): 100.0 Charged (E): 30.0 Pumped (E): 60.0
Water	500.0	Suspension: 370.0 Emulsion: 115.0	Suspension: 370.0 Emulsion: 115.0	Suspension: 400.0 Emulsion: 112.0
Sodium lauryl sulfate	3.00	2.50	2.50	2.50
Sodium bicarbonate	0.50	0.30	0.30	0.30
Potassium persulfate	0.50	0.30	0.30	0.30
Poly(vinyl alcohol)	—	3.00	2.00	2.20
Benzoyl peroxide	—	4.00	4.00	4.00

Components	Operation conditions			
	REAC01	REAC04	REAC05	REAC06
Temperature (°C)	85.0	85.0	85.0	85.0
Agitation speed (rpm)	600 ± 50	1500 ± 50	1080 ± 50	1100 ± 50
Impeller (type)	01	01	02	01
Feed time (min)	40	120	120	120

In the Water row, the terms *suspension* and *emulsion* indicate the amount of the component used in each polymerization system, respectively. The symbol *S* refers to the suspension polymerization and *E* refers to the emulsion polymerization. Impeller type 01 was formed by six plane blades with 45° between each blade, and type 02 was a marine propeller. *Charged* refers to the amount of monomer used at the beginning of the reaction, and *pumped* refers to the amount of monomer pumped along the experimental run.

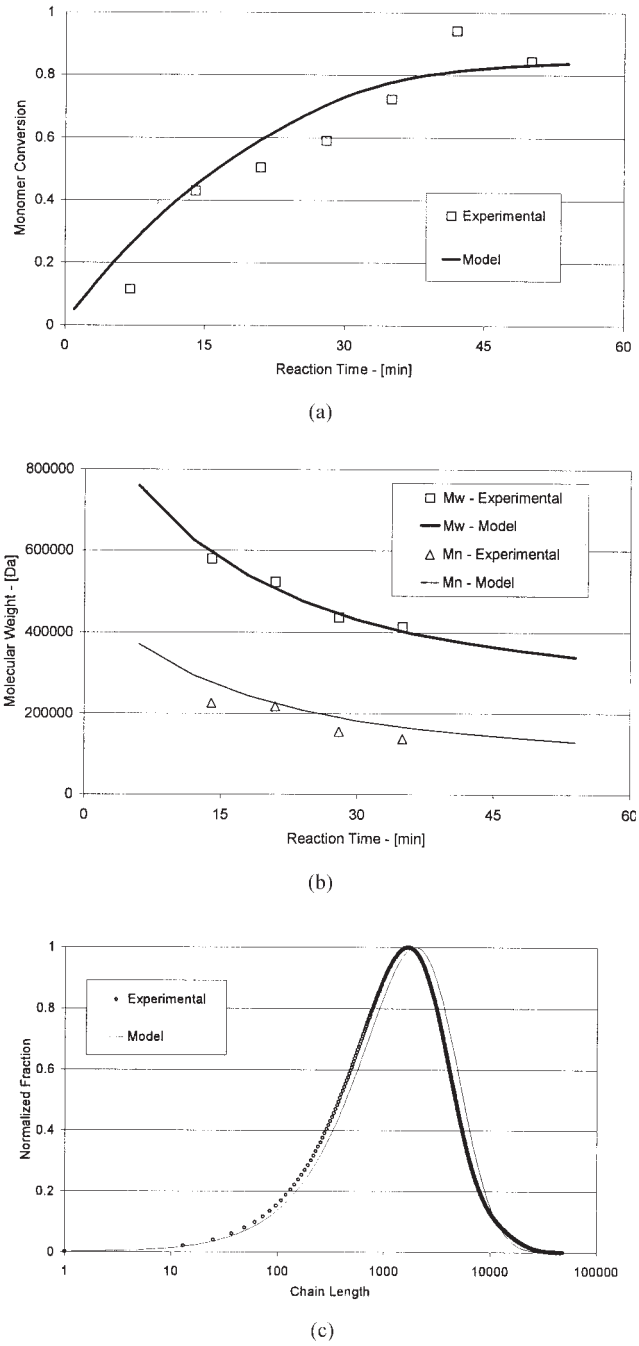

Figure 2 Comparison of experimental and modeling results of the (a) monomer conversion, (b) molecular weight averages, and (c) MWD at the instant $t = 21$ min for REAC01.

lower the surface area will be for a constant monomer holdup. Therefore, lower k_{NP} values should be expected for bigger particles.

2. k_{NP} depends on the monomer conversion inside the polymer particles formed by the suspension polymerization process. As the monomer conversion increases above the particle identification point (ca. 60–70%), the polymer particles become more rigid and less subject to agglomeration. Therefore, higher k_{NP} values should be expected for lower monomer conversions.

RESULTS AND DISCUSSION

This section compares the experimental data reported by Lenzi et al.[23] with simulation data obtained with the proposed mathematical models. First, the conventional emulsion polymerization process is analyzed. Then, the conventional suspension polymerization is analyzed with the experimental data obtained during the first step of the semibatch suspension process. The experimental data obtained for reaction runs REAC01, REAC05, REAC06, and REAC07, as reported by Lenzi et al.,[23] were used for modeling purposes. REAC01 was a typical semibatch styrene emulsion polymerization. REAC05 and REAC06 were semibatch suspension polymerizations where the constituents of the emulsion process were added 2 h after the start of the conventional suspension process. Finally, REAC07 was a semibatch suspension polymerization where the constituents of the emulsion process were added 4 h after the startup of the conventional suspension process. These experimental runs led to the simultaneous

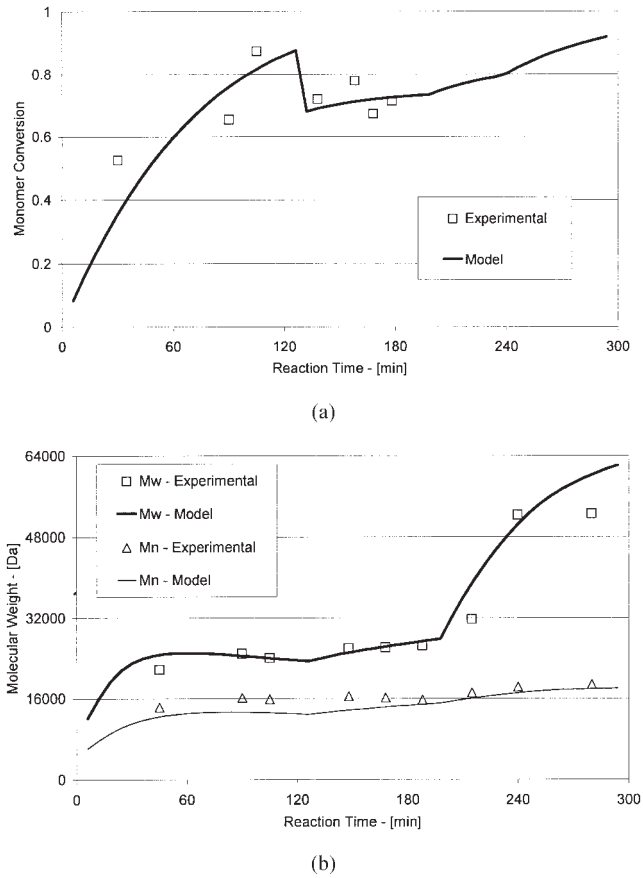

Figure 3 Comparison of experimental and modeling results of the (a) monomer conversion and (b) molecular weight averages for REAC05.

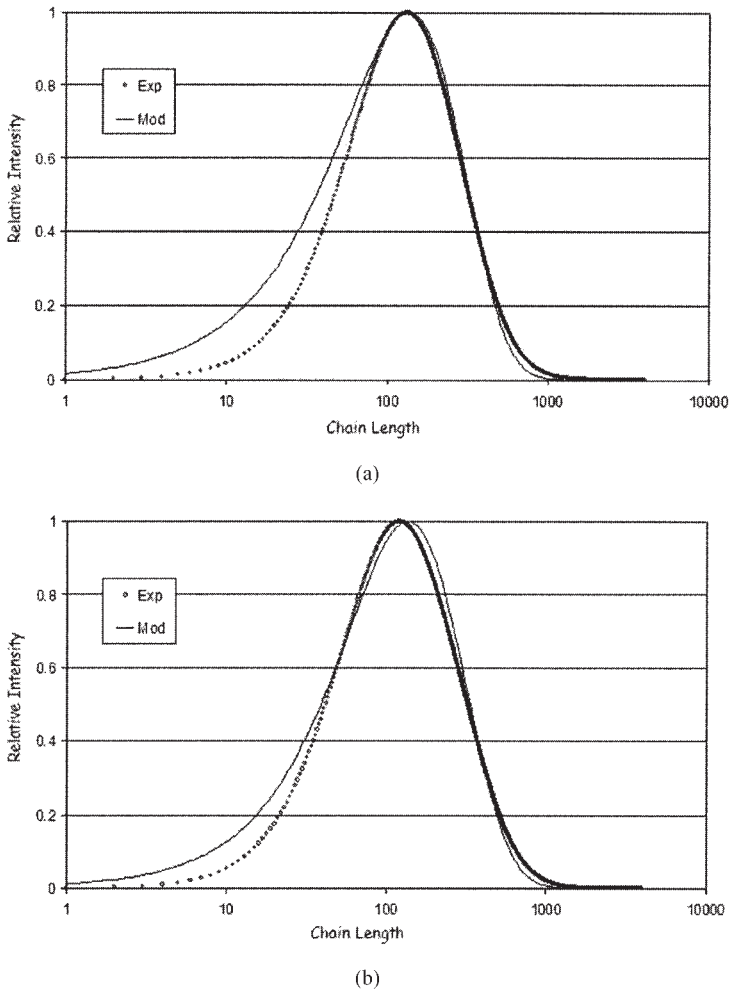

Figure 4 Comparison of experimental and modeling results of the MWDs at the instants t = (a) 90 and (b) 168 min for REAC05.

formation of the core–shell morphology and of polymer resins with broad MWDs. Further details regarding the experimental procedure and product characterization techniques can be found in Lenzi et al.[23] Table V presents the polymerization recipes of the experimental runs used for the modeling studies.

Emulsion polymerizations

Table V shows the polymerization recipe of REAC01. Approximately 43% of the monomer was loaded at the beginning of the reaction, whereas the remaining 57% of the monomer was fed into the reaction vessel along the run at a constant feed rate of 1 g/min. Figure 2(a) compares the evolution of the experimental and simulated monomer conversion data. High monomer conversion was achieved in less than 1 h, and there was fair agreement between the experimental and simulation results. The evolution of simulated and experimental molecular weight averages are shown in Figure 2(b). Very high molecular weights were achieved. As all of the chemicals were used as received, impurities and chain-transfer agents accumulated linearly during the feed time. To take this effect into account, chain transfer rates were assumed to increase linearly and proportionally with the monomer feed. This explains the continuous decrease in the molecular weight averages. Figure 2(c) shows that the MWD of the polymer was also described extremely well by the model. All of these results indicate that model assumptions used to describe the emulsion polymerization process could be regarded as very good.

Semibatch suspension polymerizations

The semibatch suspension polymerizations comprise two distinct steps. The first step is a conventional batch suspension polymerization process. The second step is initiated when the constituents of a typical emulsion polymerization recipe are added into the reaction vessel. Table V shows the polymerization recipes for runs REAC05, REAC06, and REAC07. The

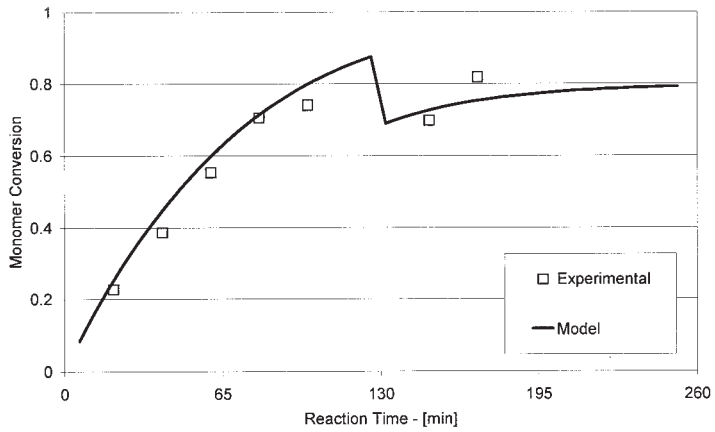

(a)

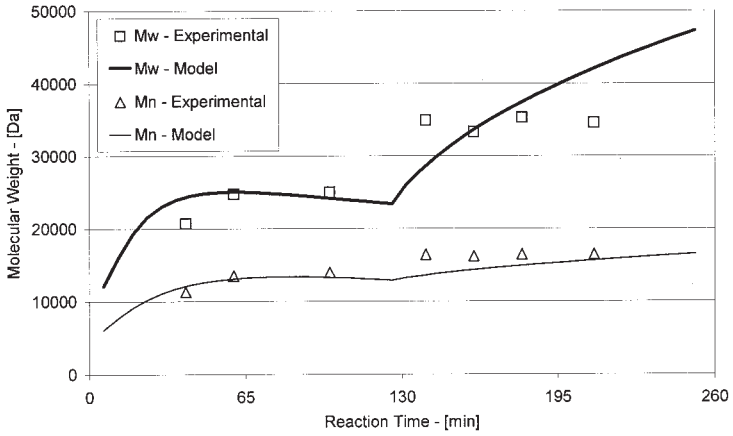

(b)

Figure 5 Comparison of experimental and modeling results of the (a) monomer conversion and (b) molecular weight averages for REAC06.

experiments were designed to allow for analysis of the effects of both monomer conversions and average droplet size on the reaction course. Despite the similar recipes, REAC05 and REAC06 were performed at different mixing conditions to produce polymer particles of different sizes. On the other hand, REAC05 and REAC07 were performed at similar mixing conditions; however, in REAC05, the constituents of the emulsion polymerization process were added 2 h after the startup of the suspension polymerization reactions, whereas in REAC07, this addition was performed 4 h after the startup of the suspension reaction.

Figures 3–8 compare the experimental and simulation data obtained for REAC05, REAC06, and REAC07. The only adjusted parameter was k_{NP}, which was assumed to be constant along the run. Different k_{NP} values were estimated for each run, as described previously.

Immediately before the initiation of the feeding of the emulsion constituents, the polymer particles of experimental run REAC05 presented an average diameter of 50 μm. The comparison between experimental data and model results is shown in Figures 3 and 4. Figure 3(a) shows the evolution of monomer conversions, whereas Figure 3(b) compares the evolution of molecular weight averages. A good agreement between experimental data and model predictions was achieved. An increase in the M_w was observed after the addition of the constituents of the emulsion polymerization process. The estimated value of k_{NP} was equal to 2 s^{-1}. As the average particle size before the addition of the constituents of the emulsion charge was small, a relatively high surface area was available for particle agglomeration. To confirm this observation, the gravimetrical analysis of the solid content of the supernatant of the final latex indicated that just 0.3% of the polymer material remained emulsified in the aqueous phase, indicating the high efficiency of the agglomeration process. Model predictions gave support to the assumption of the loss of compartmentalization after agglomeration of the emulsion polymer particle and the suspension polymer particle. This

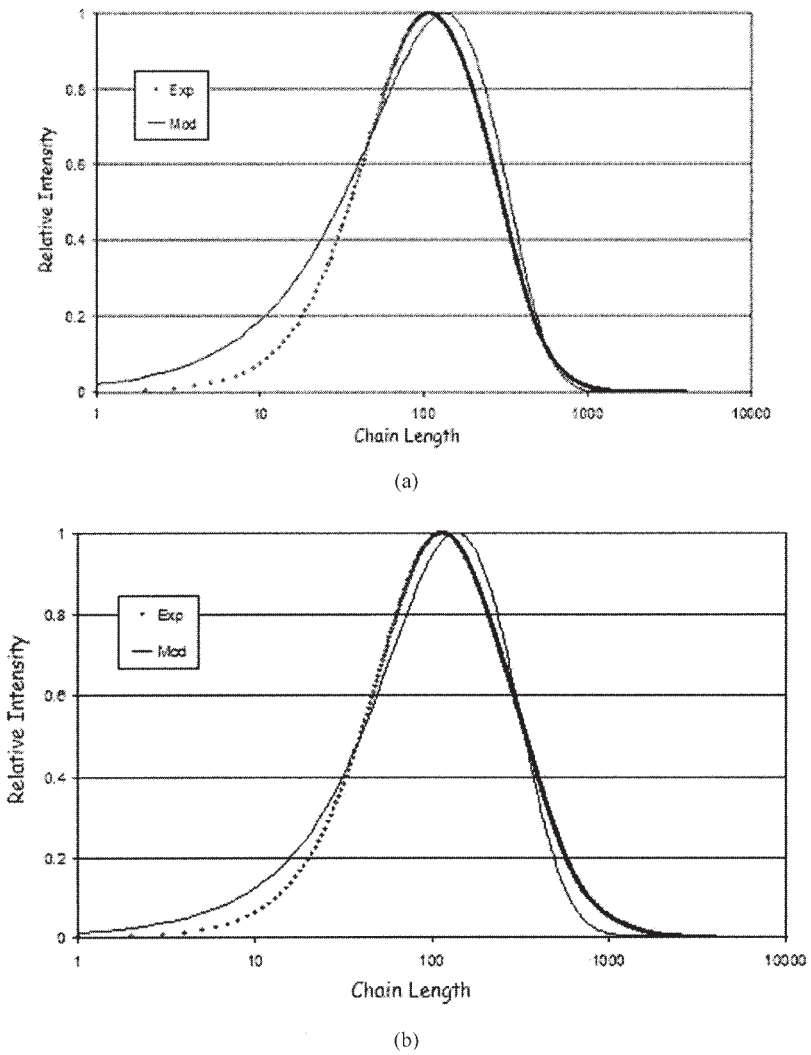

Figure 6 Comparison of experimental and modeling results of the MWDs at the instants t = (a) 100 and (b) 180 min for REAC06.

hypothesis was also supported by the small increase in the molecular weight averages after the addition of the emulsion polymerization charge. Although Figure 1 shows that M_w values of 500,000 Da were obtained during the emulsion process, M_w of the polymer resin increased from 20,000 Da to only 50,000 Da after the addition of the emulsion process charge during the semibatch suspension process. This can be understood if one realizes that polymerization conditions inside the emulsion particles after agglomeration were similar to the polymerization conditions inside the suspension particles due to the loss of compartmentalization and mass transfer between phases I and III.

A comparison between the experimental and simulation MWD data is shown in Figure 4 for REAC05. The analysis of the polymer resin in the reaction vessel 30 min before the addition of the emulsion process charge is presented in Figure 4(a). Figure 4(b) presents the analysis 48 min after the startup of emulsion feeding. Again, good agreement between experimental data and model predictions was observed, although the low-molecular-weight side of the distribution presented some discrepancy.

Polymer particles of experimental run REAC06 presented an average size of 550 μm immediately before the addition of the emulsion process charge. Particle sizes were much larger in this case because of the different agitator impeller used in the experiment. As in suspension polymerizations, the kinetic behavior did not depend on the particle size; the monomer conversions of REAC05 and REAC06 were roughly the same immediately before the addition of the constituents of the emulsion polymerization process. For this reason, the influence of the particle size could be accurately assessed. A comparison between the experimental and simulation results for REAC06 is shown in Figures 5 and 6. Figure 5(a) shows the evolution of the monomer conversion, whereas Figure 5(b) compares the evolution of molecular weight averages. Fair agreement between experimental data and model re-

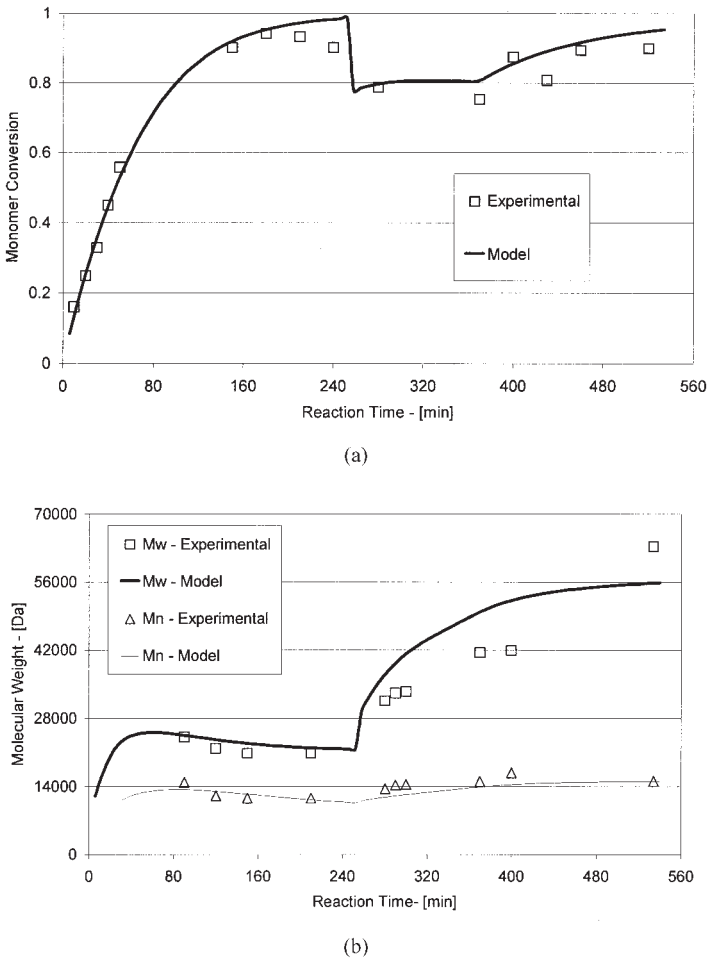

Figure 7 Comparison of experimental and modeling results of the (a) monomer conversion and (b) molecular weight averages for REAC07.

sults was also achieved. Similar to REAC05, an increase in the molecular weight averages was observed after the addition of the constituents of the emulsion polymerization process. A higher increase in the molecular weight averages was observed for REAC06 when compared to REAC05, due to the slower agglomeration process. As a consequence, higher amounts of polymer were produced by the emulsion polymerization, leading to a polymer with a higher molecular weight. With the experimental data of REAC06, the value adjusted for k_{NP} was equal 0.01 s^{-1}, which confirmed the lower rates of agglomeration. This value was lower than the value of k_{NP} adjusted for REAC05. The main reason was the lower surface area available for particle agglomeration, as the monomer conversion of the suspended droplets before feeding of the emulsion recipe was roughly the same. It was very interesting to observe that particles in REAC06 were about 10 times larger than particles in REAC05, which meant that the interfacial area was about 100 times smaller in REAC06 than in REAC05. The values of k_{NP} followed this trend very clearly, indicating that agglomeration was probably proportional to the interfacial area. In REAC06, the final efficiency of the agglomeration process was also very high, as the gravimetrical analysis of the solid contents of the supernatant of the final product revealed that just 1.5% of polymer material remained emulsified in the aqueous phase.

A comparison between the experimental and simulation MWD data is shown in Figure 6. An analysis of the polymer resin in the reaction vessel 20 min before the addition of the emulsion process charge is presented in Figure 6(a). Figure 4(b) presents the analysis 60 min after the startup of emulsion feeding. Again, good agreement between the experimental data and the model output was observed.

In REAC07, the constituents of the emulsion polymerization recipe were added only 4 h after the startup of the suspension process. Consequently, the monomer conversion of the polymer beads of REAC07 was higher than in REAC05, when addition of the emulsion process charge was started. It seems correct to assume that if the monomer conversion had no influence over the agglomeration process, the adjusted value of k_{NP} for experimental run REAC07 would

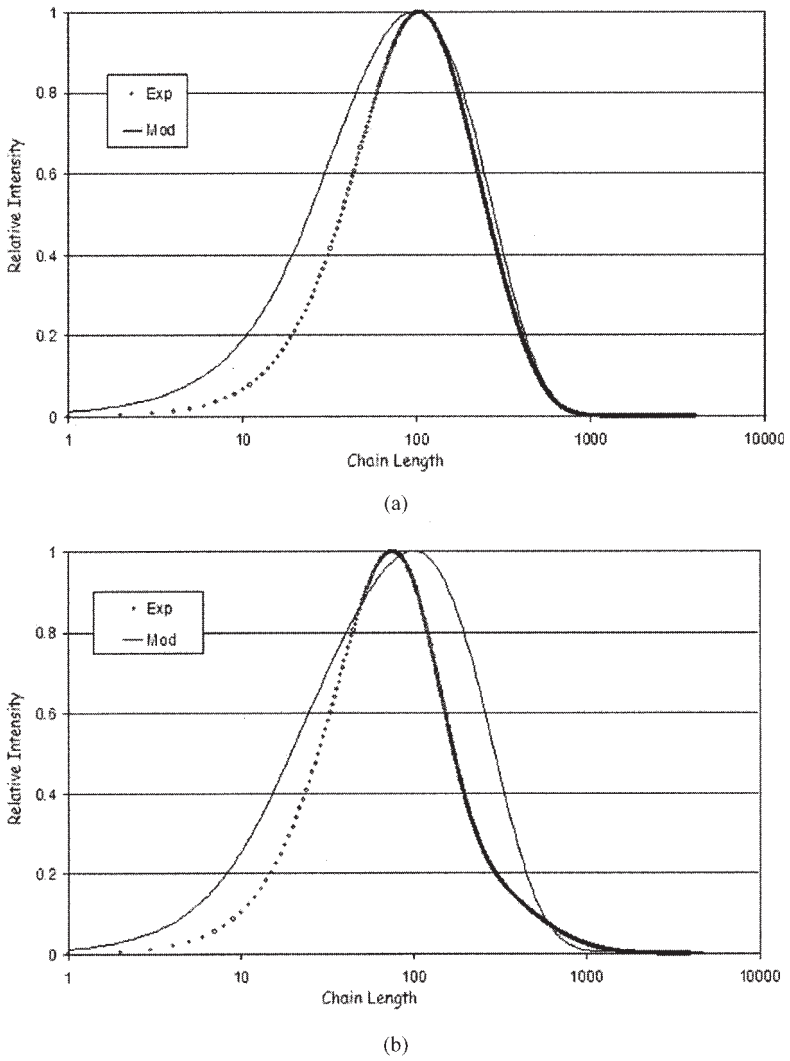

Figure 8 Comparison of experimental and modeling results of the MWDs at the instants t = (a) 90 and (b) 280 min for REAC07.

have to have been similar to the value obtained for REAC05, due to the similar particle sizes. However, the adjusted value of k_{NP} for REAC07 was equal to 2×10^{-4} s^{-1}, which was considerably lower than the value adjusted for REAC05 ($2\ s^{-1}$). Thus, it is possible to conclude that the monomer conversion of the polymer particle produced by the suspension process played a key role in the agglomeration of the emulsified polymer particles. This happened because the particles became more rigid and less sticky when the monomer conversion of the polymer beads increased. Therefore, higher agglomeration rates of the emulsion polymer particles should be expected to take place when monomer conversion is lower. A comparison between the experimental and simulation data for REAC07 is shown in Figures 7 and 8. Figure 7(a) shows the evolution of the monomer conversion, whereas Figure 7(b) compares the evolution of the molecular weight averages. Good agreement between the experimental data and the model predictions was achieved. An increase in the molecular weight averages after the addition of the emulsion polymerization process was also observed. The increase in the molecular weight averages was higher in REAC07 than observed previously in REAC05 and REAC06 due to the much lower agglomeration rates, which allowed for higher amounts of polymer chains to be produced by the emulsion polymerization process. Although the polymer particles were not as sticky as in REAC05 and REAC06, the gravimetrical analysis of the solid contents of the supernatant of the final product revealed that just 1.5% of the overall polymer material remained in the emulsified form, indicating an efficient agglomeration process. This fact was also confirmed by the formation of the core–shell structure.

A comparison of MWD data is shown in Figure 8. The analysis of the polymer resin in the reaction vessel 30 min before the addition of the emulsion process

charge is presented in Figure 8(a). On the other hand, Figure 8(b) presents the analysis after 40 min of simultaneous reaction. Good agreement between experimental data and model predictions was observed.

The obtained results indicate that k_{NP} may have experienced dramatic changes along a particular run, given the extremely different results evaluated for k_{NP} in REAC05 and REAC07. Therefore, the estimated k_{NP} values should be regarded as average values that can represent the average behavior of the run. The computed MWD values were always broader than the experimental values, which may be an indication that phases I and III presented very similar chemical compositions and that rates of mass transfer were very high between the core and the shell of the particles. These effects should be analyzed more deeply in future investigations. Despite that, the mathematical model presented here was able to describe the main features of the semibatch suspension process used for the production of the core–shell polymer particles.

CONCLUSIONS

A mathematical model for the semibatch styrene suspension polymerization process proposed by Lenzi et al.[23] was developed and validated with experimental data. We developed the mathematical model was developed by linking a previously validated suspension polymerization process model to an emulsion process polymerization model by considering the agglomeration of emulsified and suspended polymer particles, which is responsible for the formation of the core–shell structure. When the agglomeration phenomenon was considered a first-order process and the parameter k_{NP} was considered a step function, the experimental data fit fairly well. It was also shown that the agglomeration rate depended on the following variables:

1. The degree of conversion of polymer particles formed by the suspension polymerization process: the lower the initial conversion was, the higher the rates of agglomeration were.
2. The size of the polymer particles formed by the suspension polymerization process: the bigger the particle size was, the smaller the total contact area with the emulsion particles was and the lower the rates of agglomeration were.

The authors thank CAPES, CNPq, and FAPERJ (Brazilian Agencies) and Queen's University for scholarships and financial support. The authors also thank Nitriflex Resinas SA for providing chemicals.

NOMENCLATURE

a_{mic}	Surface area of a micelle (cm^2)
a_{mon-AQ}	Interfacial area between the aqueous phase and the monomer droplets in the emulsion polymerization process (cm^2)
a_P	Surface area of a polymer particle of the emulsion polymerization process (cm^2)
a_{I-III}	Interfacial area between phases I and III (cm^2)
a_{II-V}	Interfacial area between phases II and V (cm^2)
a_{III-V}	Interfacial area between phases III and V (cm^2)
a_{IV-V}	Interfacial area between phases IV and V (cm^2)
$a_{Part-AQ}$	Interfacial area between the polymer particle and the aqueous phase and monomer droplets in the emulsion polymerization process (cm^2)
cmc	Critical micelle concentration (g/cm^3)
f_{emu}	Water-soluble initiator efficiency
f_{susp}	Oil-soluble initiator efficiency
i	Chain length
i	Number-average chain size of the MWD of live polymer chains, calculated in terms of the leading statistical moments
[I]	Initiator concentration (mol/L)
$[I^{\phi}]$	Initiator concentration in the phase ϕ, where ϕ is I or III (if the superscript EQ is present, this indicates the equilibrium monomer concentration in the phase indicated by the mass-transfer coefficient; mol/L)
I	Number of moles of initiator
I^{ϕ}	Number of moles of initiator in the phase ϕ, where ϕ is I, III, or V
k_d^{susp}	Oil-soluble initiator decomposition rate constant (1/s)
k_d^{emu}	Water-soluble initiator decomposition rate constant (1/s)
ki_{I-III}	Oil-soluble initiator mass-transfer coefficient between phases I and III (cm/s)
km_{I-III}	Monomer mass-transfer coefficient between phases I and III (cm/s)
km_{II-V}	Monomer mass-transfer coefficient between phases II and V (cm/s)
km_{III-V}	Monomer mass-transfer coefficient between phases III and V (cm/s)
km_{IV-V}	Monomer mass-transfer coefficient between phases IV and V (cm/s)
km_{mon-AQ}	Monomer mass-transfer coefficient between the monomer droplets and aqueous phase in the emulsion polymerization process (cm/s)
$km_{Part-AQ}$	Monomer mass-transfer coefficient between the polymer particles and aqueous phase in the emulsion polymerization process (cm/s)

k_{NP} Parameter of the emulsion polymer particle agglomeration process (1/s)
k_P Propagation rate constant ($cm^3\ mol^{-1} \cdot s^{-1}$)
k_{tf_mon} Chain transfer to monomer rate constant ($cm^3\ mol^{-1} \cdot s^{-1}$)
k_{t_comb} Termination by combination rate constant ($cm^3\ mol^{-1} \cdot s^{-1}$)
[M] Monomer concentration (mol/cm^3)
$[M^{\phi}]$ Monomer concentration in the phase ϕ, where ϕ is I, II, III, IV, or V (if the superscript EQ is present, this indicates the equilibrium monomer concentration in the phase indicated by the mass-transfer coefficient; mol/cm^3)
$[M_{\phi}]$ Monomer concentration in the phase ϕ, where ϕ is the monomer, polymer particles, or aqueous phase (if the superscript EQ is present, this indicates the equilibrium monomer concentration in the phase indicated by the mass-transfer coefficient; mol/cm^3)
M Number of moles of monomer
M_{FEED} Monomer feed flow rate (mol/s)
M^{ϕ} Number of moles of monomer in the phase ϕ, where ϕ is I, II, III, IV, or V
M_{ϕ} Number of moles of monomer in the phase ϕ, where ϕ is the monomer, polymer particles, or aqueous phase
mic Micelle
M_n Number-average molecular weight (g/mol)
M_w Weight-average molecular weight (g/mol)
n Chain length
n Average number of growing radicals per particle of the emulsion polymerization process
N_A Avogadro's number
N_{mic} Number of micelles
N_P Number of polymer particles formed in the emulsion polymerization process
P_i Number of moles of growing polymer radicals with a chain size equal to i
P_i^{ϕ} Number of moles of growing polymer radicals with a chain size equal to i in the phase ϕ, where ϕ is I, II, or III
Part Polymer particle of the emulsion process containing no growing polymer chains
PM_{mon} Monomer molecular weight (g/mol)
q Flory's probability of propagation
q^{ϕ} Flory's probability of propagation in the phase ϕ, where ϕ is I, II, or III
$R\cdot$ Radical formed by initiator decomposition
$R\cdot^{\phi}$ Radical formed by initiator decomposition in the phase ϕ, where ϕ is I, III, or V
r_P^{susp} Propagation rate of the bulk/suspension polymerization process (mol $cm^{-3} \cdot s^{-1}$)
$r_P^{susp-\phi}$ Propagation rate of the bulk/suspension polymerization process in the phase ϕ, where ϕ is I or III (mol $cm^{-3} \cdot s^{-1}$)
r_P^{emu} Propagation rate of the emulsion polymerization process (mol $cm^{-3} \cdot s^{-1}$)
t Time (s)
V^{ϕ} Volume of the phase ϕ, where ϕ is I, II, III, IV, or V (cm^3)
V_{ϕ} Volume of the phase ϕ, where ϕ is the aqueous phase, monomer, or polymer particles (cm^3)
V_{org} Volume of the organic phase of the suspension/bulk polymerization process (cm^3)
V_{Pol} Volume of the polymer phase of the emulsion polymerization process (cm^3)

Greek symbols

Θ Number of moles of polymer
Θ_i Number of moles of polymer chains with chain length i
Θ_i^{ϕ} Number of moles of polymer chains with chain length i in the phase ϕ, where ϕ is I, II, or III
Θ_i^{final} Number of moles of polymer chains with chain length i in the final product of the semibatch suspension process
χ Monomer conversion
ϕ System phase
λ_k kth-order moment of the dead polymer chain distribution
λ_k^{ϕ} kth-order moment of the dead polymer chain distribution in the phase ϕ, where ϕ is I, II, or III
μ_k kth-order moment of the growing polymer chain distribution
μ_k^{ϕ} kth-order moment of the growing polymer chain distribution in the phase ϕ, where ϕ is I, II, or III

References

1. Vicente, M.; Benamor, S.; Gugliotta, L. M.; Leiza, J. R.; Asua, J. M. Ind Eng Chem Res 2001, 40, 218.
2. Sayer, C.; Lima, E. L.; Pinto, J. C.; Arzamendi, G.; Asua, J. M. Comput Chem Eng 2001, 25, 839.
3. Maschio, G.; Bello, T.; Scali, C. Chem Eng Sci 1994, 49, 5071.
4. Soares, J. B. P.; Kim, J. D. J Polym Sci Part A: Polym Chem 2000, 38, 1408.
5. Aris, R. Chem Eng Sci 1993, 48, 2507.
6. Dotson, N. A.; Galvan, R.; Laurence, R. L.; Tirrell, M. Polymerization Process Modeling; VCH: New York, 1995.
7. Latado, A.; Embiruçu, M.; Neto, A. G. M.; Pinto, J. C. Polym Test 2001, 20, 419.
8. Santos, A. F.; Lima, E. L.; Pinto, J. C.; Graillat, C.; McKenna, T. J Appl Polym Sci 2003, 90, 1213.
9. Crowley, T. J.; Choi, K. Y. Chem Eng Sci 1998, 53, 2769.

10. Zaldivar, C.; Iglesias, G.; del Sol, O.; Pinto, J. C. Polymer 1997, 38, 5823.
11. Yuan, H. G.; Kalfas, G.; Ray, W. H. J Macromol Sci Rev Macromol Chem Phys 1991, 31, 215.
12. Kalfas, G.; Yuan, H.; Ray, W. H. Ind Eng Chem Res 1993, 32, 1831.
13. Kalfas, G.; Ray, W. H. Ind Eng Chem Res 1993, 32, 1822.
14. Machado, R. A. F.; Pinto, J. C.; Araújo, P. H. H.; Bolzan, A. Braz J Chem Eng 2000, 17, 395.
15. Vivaldo-Lima, E.; Wood, P. E.; Hamielec, A. E.; Penlidis, A. Ind Eng Chem Res 1997, 36, 939.
16. Gao, J.; Penlidis, A. Prog Polym Sci 2002, 27, 403.
17. Harkins, W. D. J Chem Phys 1945, 13, 381.
18. Vanderhoff, J. W. Chem Eng Sci 1993, 48, 203.
19. Araujo, O.; Giudici, R.; Saldívar, E.; Ray, W. H. J Appl Pol Sci 2001, 79, 2360.
20. Smith, W. V.; Ewart, R. H. J Chem Phys 1948, 16, 592.
21. Min, K. W.; Ray, W. H. J Macromol Sci Rev Macromol Chem Phys 1974, 11, 11.
22. Saldivar, E.; Dafniotis, P.; Ray, W. H. J Macromol Sci Rev Macromol Chem Phys 1998, 38, 207.
23. Lenzi, M. K.; Silva, F. M.; Lima, E. L.; Pinto, J. C. J Appl Polym Sci 2003, 89, 3021.
24. Gentric, C.; Pla, F.; Latifi, M. A.; Corriou, J. P. Chem Eng J 1999, 75, 31.
25. Gilbert, R. Emulsion Polymerization A Mechanistic Approach; Academic: London, 1995.
26. Ray, W. H. J Macromol Sci Rev Macromol Chem Phys 1972, 8, 01.
27. Kiparissides, C.; Seferlis, P.; Mourikas, G. Ind Eng Chem Res 2002, 41, 6120.
28. Flory, P. J. Principles of Polymer Chemistry; Cornell University Press: Cornell, NY, 1953.
29. Petzold, L. R. A Description of DASSL: A Differential Algebraic System Solver; Report # SAND82–8637; Sandia National Laboratories: Livermore, CA, 1982.
30. Brandrup, J.; Immergut, E. H.; Grulke, E. A. Polymer Handbook; Wiley: New York, 1999.